Some Impulsive Rendezvous Trajectories and their Possible Optimality

J. P. PELTIER*
Princeton University, Princeton, N.J.

Two- and three-impulse trajectories are investigated for fixed-time, fixed-angle rendezvous between vacant circular coplanar orbits, for trip angles less than, or equal to 2π in magnitude. For two-impulse trajectories, general features of the characteristic velocity function are outlined. Parameters of the intermediate orbit are reviewed. Attention is given to limiting cases. Computation of the adjoint system helps to define the domain of possible optimality for such trajectories: it is a closed domain in the trip time, trip angle plane. Waiting periods on terminal orbits are considered. The domain of possible optimality is defined using Lawden's primer vector theory. This domain extends to infinity if the radius ratio of terminal orbits is less than 15.6. Three-impulse trajectories are tried in cases where two-impulse trajectories, with or without coast, have been found nonoptimal. Improvements on the characteristic velocity are thus obtained.

Nomenclature

Symbols

H	= Hohmann trajectory
T	= thrust or impulse
C_0	= coast, including zero complete revolution
(C)	= optional coast with unprecised number of revolutions
TC_0T	= two-impulse trajectory
$(C)TC_0T(C)$	= two-impulse trajectory with optional terminal coast
O	= center of inverse-square gravitational field
$(PO)_n$	= domain of possible optimality for n-impulse trajectories
$(PO)_{n+}$	= domain of possible optimality for n-impulse + terminal coast trajectories

Variables

E	= energy
e	= eccentricity
$\mathbf{G}$	= gravity gradient matrix
H	= Hamiltonian $= \mathbf{\Lambda}\cdot\ddot{\mathbf{x}}-\dot{\mathbf{\Lambda}}\cdot\dot{\mathbf{x}}$
$\mathbf{h}$	= angular momentum
J	= performance index, equal to the characteristic velocity Δv
$\mathbf{k}$	= out-of-plane unit vector
k	= integer
p	= magnitude of the primer vector $= (\mathbf{\Lambda}\cdot\mathbf{\Lambda}^T)^{1/2}$
r_1	= radius of the inner circular terminal
r_2	= radius of the outer circular terminal
r_3	= distance from departure to arrival point $= (r_1^2+r_2^2-2r_1r_2\cos\phi)^{1/2}$
t	= current time
v	= velocity, in rectilinear cases
$\mathbf{x}$	= position vector
Δv	= characteristic velocity
Φ	= total trip angle, counted planetwise
$\mathbf{\Lambda}$	= primer vector
λ_θ	= out-of-plane component of vector $\dot{\mathbf{\Lambda}}_\Lambda\mathbf{x}-\mathbf{\Lambda}_\Lambda\dot{\mathbf{x}}$
μ	= gravitational constant
ρ	= radius ratio $= r_2/r_1 \geqq 1$.
τ	= total trip time
θ	= true anomaly, counted planetwise from pericentron
ψ	= thrust impulse, counted counter-planetwise from local horizontal
ω	= angular velocity $= \dot{\theta}$

Subscripts

m	= minimum characteristic velocity
p	= parabolic intermediate trajectory
r	= radial intermediate trajectory
1, 2	= inner, outer terminal impulse

Received January 19, 1971; revision received September 20, 1971. This paper is based upon the author's MSE thesis at Princeton University, Department of Aerospace and Mechanical Sciences. P. M. Lion and M. Handelsman are most gratefuly thanked for the benefit of their unstinted advice. This work has been supported by NASA Grant NGR 31-001-152 and part of the computations by National Foundation Grants NSF-gJ-34 and NSF-GU-3157.

Index category: Lunar and Planetary Trajectories.

* Graduate Student; presently with ONERA, Châtillon-sous-Bagneux, France.

Introduction

INCREASING remoteness of space exploration objectives and increasing sophistication of space probes are factors that enhance interest in controlled space trajectories, among which impulsive trajectories are of prime practical and theoretical importance. The work presented here is directed primarily toward possible interplanetary applications. In such a case it is not possible to contemplate neighboring terminal orbits (thus, the problem will be nonlinear) and multiple-loop trajectories can be, in a first approach, barred from consideration (mainly for reason of trip time, although infinite trip times will be considered here for completeness). Thus, the problem is that of nonlinear rendezvous (and not transfers) which means, except for a few simple cases, that a closed-form analysis is not available and numerical methods are used. This is true not only for the determination of candidate trajectories but also for the study of their possible optimality.

A basic problem arising in the computation of rendezvous trajectories is the Lambert's problem,[1]† which is, by now, well known. An introduction to it can be found in Breakwell et al.,[2] or Jordan.[3] Numerical methods have been developed by Pines,[4] Battin,[5] and other authors. An interesting feature of the problem is the uniqueness of the solution providing that the intermediate coasting arc does not duplicate state variables (i.e. has less than one period). This copes very well with what has been said above about multiple-loop trajectories where the trip angle is restrained to be $|\Phi| \leqq 2\pi$. It ensures that one two-impulse trajectory exists for any set of the variables τ, ϕ, ρ. This is why two-impulse trajectories can be extensively scrutinized. In order to keep the number of independent parameters down to three, terminal orbits have been chosen to be circular and coplanar.

The present work can be regarded as being in three different, although unequal, parts.

1) A complete description of two-impulse TC_0T trajectories is given. This includes parameters of the intermediate orbit (an extension to Jordan's[3] work on the energy) and the characteristic velocity. (It cannot be directly compared to Breakwell's results[2] which assumed inclined and elliptic terminals.)

† Reference 1 can be seen at (or copies purchased from) Bibliothèque Nationale Paris, under number 8° R22039 (133).

2) Lawden's primer vector[6] is computed along all two-impulse TC_0T trajectories and a large set is identified as nonoptimal. Conversely, what is left is a "possible optimality domain" $(PO)_2$, which is closed in the plane $\rho = \text{const}$, and extends to negative trip angle TC_0T trajectories. At this point the possibility of terminal coast is introduced at both ends of two-impulse TC_0T trajectories. The corresponding domain of possible optimality, $(PO)_{2+}$, is defined. It completes the $(PO)_2$ domain but does not overlap, as when terminal points have a nonzero mass.[7] This part is a direct extension of Handelsman's work.[8]

3) Three-impulse trajectories are tried for some of the cases where $(C)TC_0T(C)$ trajectories have been recognized as nonoptimal. Although this work did not benefit by the determining improvement presented by Lion and Handelsman[9] for multi-impulse trajectory optimization, a good evaluation of three-impulse TC_0TC_0T characteristic velocities is obtained. But the possible optimality domain $(PO)_3$ could not be defined, and this step is a prerequisite in order to find out the maximum number of impulses for all rendezvous, a problem which is solved in the linear case but not in the general case.

Results presented here are coherent with other well known results on impulsive rendezvous,[10,11,12] but comparisons cannot be readily made because, on the one hand, these works deal with the linear case [i.e., with our notations, when $\rho \to 1$ and $\phi \simeq (\omega_1+\omega_2)\pi/2$]. Prussing's study[10,11] corresponds to "small" values of ϕ (from 0 to 4π), whereas Marec's study[12] corresponds to even larger trip angles. On the other hand, the present nonlinear problem exhibits new features when $\rho \to 1$. (This case is currently under examination.) Except when noted, numerical results correspond to $\rho = 1.52$ (i.e., Earth-Mars rendezvous).

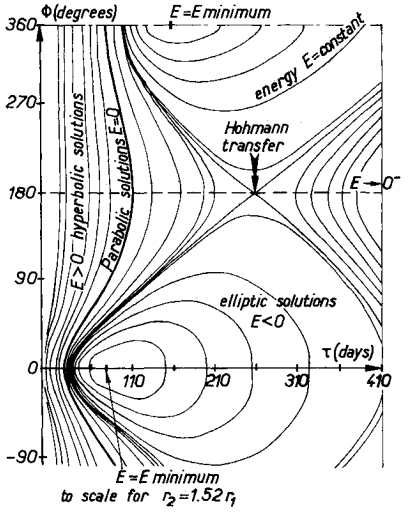

Fig. 1 Nature of Lambert's solutions (after Jordan[3]).

Geometry of Two-Impulse Trajectories

This section discusses briefly, prior to examination of the characteristic velocity and possible optimality of two-impulse TC_0T trajectories, the nature and parameters of the corresponding intermediate arcs. As recalled previously, there is a unique TC_0T trajectory for a given set of data τ, ϕ, ρ. Thus, results in this section do not depend upon terminal velocities (although a discussion for $\rho = \text{const}$ is directed toward circular terminals). Jordan,[3] in his examination of the energy of Lambert's solutions (Fig. 1) already gave much concerning the nature of these trajectories. A few precise examples will be given. Parabolic coasting arcs can be found, for finite trip times, on a single surface

$$\tau_p(|\Phi|, r_1, r_2) = [(r_1+r_2+r_3)^{3/2} - (r_1+r_2-r_3)^{3/2} \sin|\Phi|/|\sin\Phi|]/6\mu^{1/2}$$

which separates hyperbolic coasting arcs ($\tau < \tau_p$) from elliptic coasting arcs ($\tau > \tau_p$). Coasting arcs corresponding to negative ϕ are symmetric to solutions for equal positive ϕ upon the radius O-departure point. So, $E(\tau, -\phi) = E(\tau, \phi)$ and when $\phi \to 0$, $\mathbf{h} \to \mathbf{0}$, the whole coasting arc lies upon this radius,[13] with $r(t) \geqq r_1$. This kind of radial trajectory is found again on the planes $|\Phi| = 2\pi$, but then $r(t)$ may be $\leqq r_1$ and the mobile point bounces upon the center O of the field. For $\tau \to 0$, hyperbolic transfers approach their asymptotes: $E \to \infty$ and the trajectory can be described by either one segment of straight line ($|\Phi| < \pi$), or by two segments issuing from O ($|\Phi| > \pi$). Velocities along such arcs tends to infinity as $(r_2-r_1)/\tau$ or $(r_2+r_1)/\tau$. For $\tau \to \infty$, $E \to 0^-$ and the mobile point goes away to infinity and back along a parabolic coasting arc. For a given set of r_1, r_2, the energy takes its minimum value, $-\mu/r_2$, on 3 different points such that $\phi = -2\pi$, 0, $+2\pi$. The curve $E(\tau, \phi > 0) = E_H = -\mu/(r_1+r_2)$ is symmetric upon point H, as each curve $E(\tau, \phi > 0)$ is symmetric upon some point of the axis $\phi = \pi$. The eccentricity e is 1, not only when $E = 0$, but also when $\mathbf{h} = \mathbf{0}$, which makes two closed contours ($\phi \geqq 0$, $\phi \leqq 0$) inside which curves $e(\tau, \phi) = \text{const}$ close in on themselves around a minimum value $e_H = (r_2-r_1)/(r_2+r_1)$. The symmetry for $\phi > 0$ and $\phi < 0$ gives $\theta_1(\tau, -\phi) = -\theta_1(\tau, \phi)$; therefore, as when $\phi \to 0^+$, $\theta_1 \to +\pi$, when $\phi \to 0^-$, $\theta_1 \to -\pi$. For any value of ϕ other than $2k\pi$, $\theta_1(\tau, \phi)$ is monotonically increasing with τ toward an asymptotic value.

It can be noted that for a given set E, e and under the obvious condition that $r_{\min}(E, e) \leqq r_1 \leqq r_2 \leqq r_{\max}(E, e)$, the orbit thus defined intersects in two points each of the circles $r = r_1$, and $r = r_2$. There are four possible combinations of departure and arrival points, for a given sign of ϕ and for $E < 0$, therefore four set of (τ, ϕ). The number of trajectories is reduced to two if $r_{\max} = r_2$ or $r_{\min} = r_1$ and to one if both conditions are obtained (Hohmann trajectory). Similarly, if $E > 0$ there are two possible trajectories, merging if $r_{\min} = r_1$. Let τ_0 and ϕ_0 correspond to the shortest trip time, shortest trip angle trajectory among those. With $\tau_0 = t_2 - t_1$, $t = 0$ at pericentron of the orbit, and a = semimajor axis, other trajectories correspond to

$$\text{traj } 2 \begin{bmatrix} \tau = t_2+t_1 \\ \phi = \phi_0+2\theta_1 \end{bmatrix} \text{ only other solution for } E \geqq 0$$

$$\text{traj } 3 \begin{bmatrix} \tau = 2\pi a^{3/2}/\mu^{1/2} - t_2 \\ \phi = 2\pi - \phi_0 - 2\theta_1 \end{bmatrix}$$

$$\text{traj } 4 \begin{bmatrix} \tau = 2\pi a^{3/2}/\mu^{1/2} - \tau_0 \\ \phi = 2\pi - \phi_0 \end{bmatrix}$$

traj 1 being τ_0, ϕ_0. These points are the only intersection of constant E and constant e curves, and for $\theta_1 = 0$ or $\theta_1 + \phi = \pi$, $r_{\min} = r_1$ or $r_{\max} = r_2$ and the curves are tangent to each other.

Characteristic Velocity of Two-Impulse Trajectories

The characteristic velocity is defined as

$$\Delta v = \sum_{i=1}^{n} |\dot{\mathbf{x}}_i^+ - \dot{\mathbf{x}}_i^-|$$

and depends upon terminal velocities. Some special cases will be reviewed first. When $\tau \to 0$, $\Delta v \to \infty$ as $2r_3/\tau$ which is minimum, for a given τ, when $\phi = 0$. For radial trajectories, let v_2 be substituted for $\dot{\mathbf{x}}_2^-$. As $dv_2/d\tau < 0$, v_2 can replace τ as the independent variable describing solutions. The characteristic velocity is $\Delta v_r = [v_2^2 + \mu(3r_2 - 2r_1)/r_1 r_2]^{1/2} + (v_2^2 + \mu/r_2)^{1/2}$. It has a derivative $d\Delta v_2/dv_2$ of the sign of v_2, and reaches a minimum Δv_{rm} when $v_2 = 0$ (i.e., when $E = E_{\min}$; corresponding trip times are

$$\phi = 0: \quad \tau_0 = r_2^{3/2}[r_1(r_1^{-1}r_2^{-1} - r_2^{-2})^{1/2} + \text{Arctan}\,(r_2/r_1 - 1)^{1/2}]/(2\mu)^{1/2}$$

$$|\Phi| = 2\pi: \quad \tau_{2\pi} = \pi r_2^{3/2}/(2\mu)^{1/2} - \tau_0)$$

When $\tau \to \infty$, Δv_r increases toward an asymptotic value

$$\Delta v_{rp} = (3\mu/r_1)^{1/2} + (3\mu/r_2)^{1/2}$$

For parabolic transfers, the initial anomaly can be written as

$$\theta_1 = 2\,\mathrm{Arctan}\left(\{\sin\phi - [2(1-\cos\phi)/\rho]^{1/2}\}/(1-\cos\phi)\right)$$

and, with $\theta_2 = \theta_1 + \phi$, the characteristic velocity is

$$\Delta v_p(\phi) = \sum_{i=1}^{2} \{[3-2(1+\cos\theta_i)^{1/2}]\mu/r_i\}^{1/2}$$

For positive values of ϕ, this function takes a minimum value

$$\Delta v_{pm} = [(3-2^{3/2})\mu/r_1]^{1/2} + [(3-2^{3/2}\rho^{-1/2})\mu/r_2]^{1/2}$$

when $\phi = \mathrm{Arcos}(2/\rho - 1)$. It can easily be verified that $\Delta v_p(0) = \Delta v_p(\pm 2\pi) = \Delta v_{rp}$ and $\Delta v_p(-|\Phi|) = 2\Delta v_{rp} - \Delta v_p(|\Phi|)$. Note that as $\Delta v_p(\phi)$ is not constant, there are curves $\Delta v(\tau, \phi) = J$ intersecting $E(\tau, \phi) = 0$.

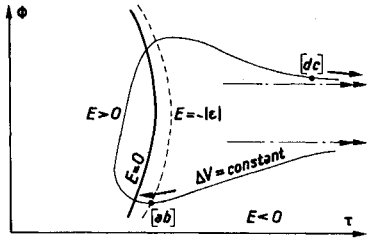

Fig. 2 Asymptotes for equal characteristic velocity curves (not to scale).

Because terminal velocities are circular velocities, the characteristic velocity is the same for the two or four trajectories defined at the end of the previous section, Therefore, the same curve $\Delta v(\tau, \phi) = J$ passes through the corresponding points and intersects there a definite set of curves $E(\tau, \phi) = \text{const}$ and $e(\tau, \phi) = \text{const}$. Moreover, that curve is tangent to these when $\theta_1(\tau, \phi) = 0$ or $\theta_2(\tau, \phi) = \pi$. Let us consider a curve $\Delta v(\tau, \phi) = J_1$, intersecting the locus $E(\tau, \phi) = 0$ at point $\tau_0{}^*$, $\phi_0{}^*$, with, at this point $(\partial E/\partial\tau)_\phi = k_1$, $(\partial E/\partial\phi)_\tau = k_2$, $(\partial\Delta v/\partial\tau)_\phi = l_1$, $(\partial\Delta v/\partial\phi)_\tau = l_2$. Let $k_3{}^2 = k_1{}^2 + k_2{}^2$ and note that $l_3 = l_2 k_1 - l_1 k_2 \neq 0$ as the two curves intersect. Let trajectory 1 defined at the end of the last section be some point of the curve $\Delta v(\tau, \phi) = J_1$, close to the locus $E(\tau, \phi) = 0$, i.e., such that $E(\tau_0, \phi_0) = -\varepsilon$ with $0 < \varepsilon \ll 1$ (Fig. 2). The corresponding trajectory 4 is found for $\tau = 2^{5/2}\pi\mu^{3/2}\varepsilon^{-3/2} - \tau_0$, $\phi = 2\pi - \phi_0$ where τ_0 and ϕ_0 can be expressed as $\tau_0 \simeq \tau_0{}^* + l_2 k_3{}^2\varepsilon/l_3$ and $\phi_0 = \phi_0{}^* - l_1 k_3{}^2\varepsilon/l_3$ for ε small enough. When $\varepsilon \to 0$, $\phi \to 2\pi - \phi_0{}^*$ while $\tau \to \infty$, therefore, the curve $\Delta v(\tau, \phi) = J_1$ has an horizontal asymptote in the plane τ, ϕ and

$$\lim_{\tau\to\infty} \Delta v(\tau, \phi) = \Delta v(E = 0, 2\pi - \phi) = \Delta v_p(2\pi - \phi)$$

The remainder of the present section is devoted to a qualitative description of the behavior of $\Delta v(\tau, \phi)$ function (Fig. 3). In order to simplify this discussion, ϕ will be regarded as defined modulo 4π. This is justified, as $\Delta v(\tau, 2\pi) = \Delta v(\tau, -2\pi)$. For $\rho > 1$, the Hohmann transfer is a minimum for the characteristic velocity of TC_0T trajectories and there are necessarily some closed contours $\Delta v(\tau, \phi) = J$ around this point. This holds for $\Delta v_H < J < \Delta v_{pm}$. For all other values of J the contours are open: for instance, on the other end of the range of values for J, when $J \geqq 2\Delta v_{rp} - \Delta v_{pm} = \max[\Delta v_p(\phi)]$, corresponding curves lie entirely in the $E > 0$ domain and they go to infinity in both directions of positive and negative ϕ; and for $\Delta v_{pm} \leqq J < 2\Delta v_{rp} - \Delta v_{pm}$, that is for the range of values covered by $\Delta v_p(\phi)$, contours have two asymptotes in the τ direction. When $J \to \Delta v_{pm}$ these two asymptotes merge into one, located at $\phi = 2\pi - \mathrm{Arcos}(2/\rho - 1)$. For $J < \Delta v_{rp}$, the asymptotes are such that $0 < \phi < 2\pi$, while for $J > \Delta v_{rp}$ they correspond to $-2\pi < \phi < 0$. Moreover, if $J < \Delta v_{rm} < \Delta v_{rp}$, the whole contour lies in the $0 < \phi < 2\pi$ domain. The last characteristic feature of the Δv function is to present a saddle point behavior for $\phi = -2\pi$, $\tau = \tau_H$. This point, noted $\bar{H}$, corresponds to a retrograde bitangent ellipse as intermediate orbit, the characteristic velocity being $\Delta v_c = (\mu/r_1)^{1/2} + (\mu/r_2)^{1/2} + [2\mu/(r_1 + r_2)]^{1/2}(\rho^{1/2} + \rho^{-1/2})$. Therefore, there are values of J $(\Delta v_c < J < 2\Delta v_{rp} - \Delta v_{pm})$ for

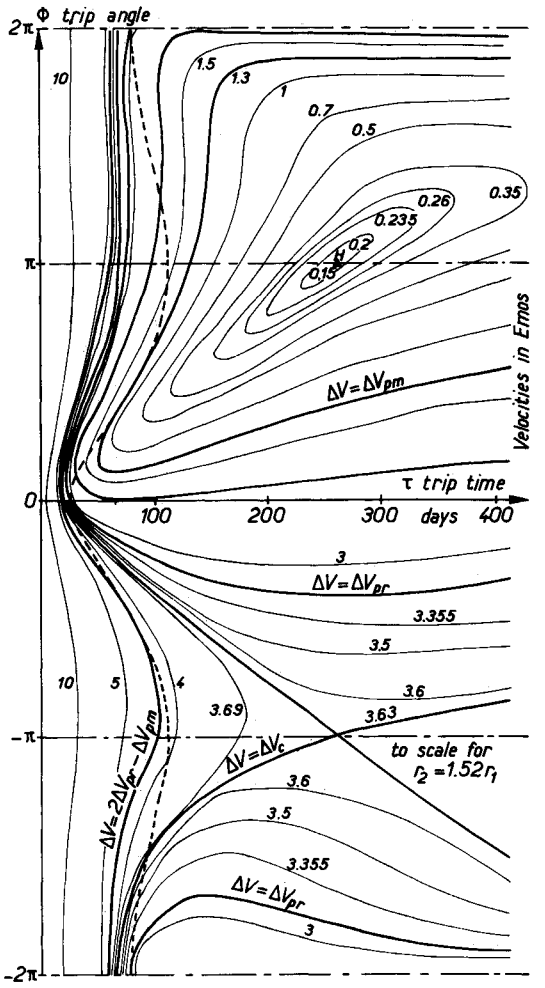

Fig. 3 Function $\Delta v(\tau, \phi)$. (EMOS = Earth mean orbital speed Δv is normalized to the initial velocity).

which the contours are not connected. They split into two distinct branches, one having two asymptotes in the τ direction, the other going to infinity in the positive and negative ϕ directions.

A final remark will be to point out that for a set of TC_0T trajectories such that $\rho > 1.25$ and the initial (final) thrust angle $\psi_1(\tau, \phi)$ $[\psi_2(\tau, \phi)]$ remains constant, the minimum Δv is obtained for a vanishing final (initial) thrust angle. But $\psi_2(\tau, \phi) = 0 \Leftrightarrow \theta_2(\tau, \phi) = \pi$ $[\psi_1(\tau, \phi) = 0 \Leftrightarrow \theta_1(\tau, \phi) = 0]$ and the curve $\psi_1(\tau, \phi) = \text{const}$ $(\psi_2 = \text{const})$ is tangent to $\Delta v(\tau, \phi) = J$ at the same point where $\Delta v = J$ is tangent to the curves of constant E and e.

Adjoint System of Two-Impulse Trajectories

Along coasting arcs, adjoint variables can be expressed in closed form (Lawden,[6] Lion and Handelsman[9]), which leaves, for a given orbit, four constants to be determined in the planar analysis. Here, the determination is made by using two necessary conditions of optimality, i.e. the primer vector Λ has to be in the direction of impulses and has to have a unit magnitude at impulse times (four conditions). Therefore, the only necessary conditions that can be violated on a coasting arc are 1) primer magnitude $p(t) \leqq 1$. for all t's and 2) $\dot{\Lambda}$ continuous at both ends of the arc. For a two-impulse TC_0T trajectory, only the first one of these conditions holds, so it will be the only test of possible optimality. But, if the problem is so easily set, a well defined $p(t)$ being attached to any TC_0T trajectory, it is not solved, yet. Even though the required constants could be formally expressed in terms of τ, ϕ and ρ (which they are not), for the general case, maxima for $p(t)$ cannot be expressed before-

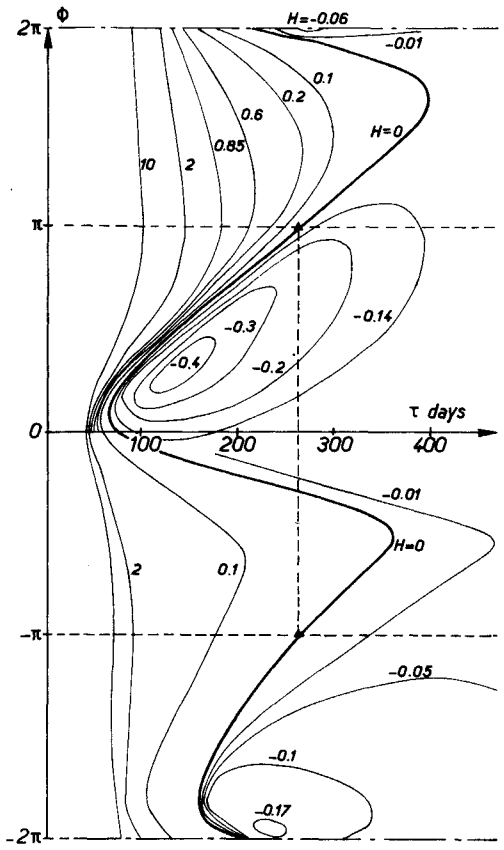

Fig. 4 The variational Hamiltonian $H(\tau, \phi)$.

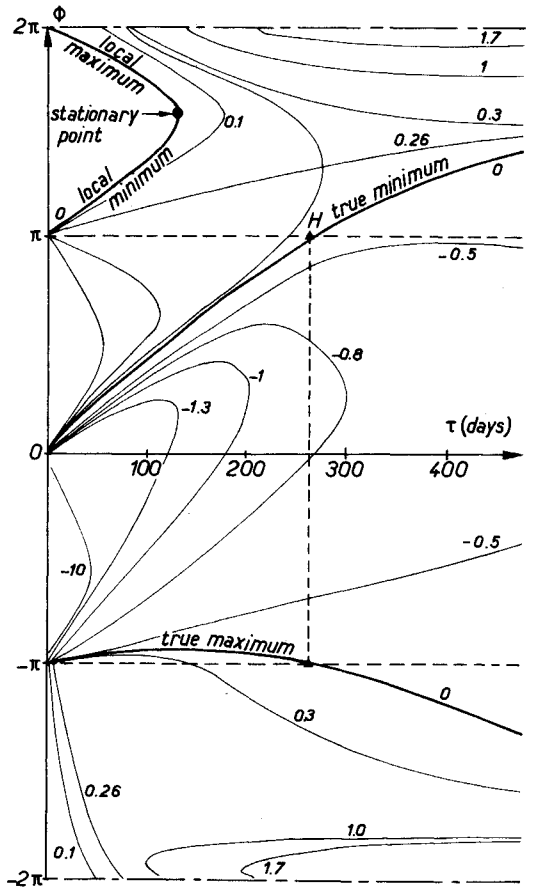

Fig. 5 Function $\lambda_\theta(\tau, \phi)$ [maxima and minima are relative to $\Delta v(\tau = \text{const}, \phi)$].

hand and $p(t)$ has to be numerically investigated. (The only attractive case is that of a circular transfer orbit for which $\mathbf{\Lambda}(t)$ is much simplified.)

Before undertaking the checking of $p(t)$, the behavior of two adjoint variables of special interest will be reviewed. The variational Hamiltonian which is associated with τ, and λ_θ, adjoint variable associated to ϕ. The first one, which can be written as $-[\partial \Delta v(\tau, \phi)/\partial \tau]_\phi$, vanishes when Δv is stationary with respect to τ, for a given ϕ. Figure 4 describes $H(\tau, \phi)$. Note how $H(\tau, \phi) = 0$ passes through the Hohmann point and through the points of minimum energy E. The second can be written as $[\partial \Delta v(\tau, \phi)/\partial \phi]_\tau$ and vanishes when Δv is stationary, with respect to ϕ, for a given trip time. Figure 5 shows $\lambda_\theta(\tau, \phi)$. Along the lines $\lambda_\theta = 0$ the nature of the behavior of $\Delta v(\tau_{\text{given}}, \phi)$ is indicated. Of course, H is of particular importance in the approach of open-time, fixed-angle transfers while λ_θ is related to fixed-time, open-angle problems. Both variables enjoy the property of being constant along the whole of any optimal multiple impulse trajectory. Anyhow, in this particular case of TC_0T trajectories, they are uniquely defined [through $\mathbf{\Lambda}(t)$] for any trajectory, optimal or not.

The expressions of H and λ_θ given above show that **grad** $[\Delta v(\tau, \phi)] = (-H, \lambda_\theta)$; therefore, a vector tangent to the curve $\Delta v(\tau, \phi) = J$ is given by (λ_θ, H) and the slope of the tangent, in (τ, ϕ) axis, is H/λ_θ. This quantity is related to the sign of $\dot{p}(t)$ at impulse points.[8] This relation can be expressed by

a) if $\lambda_\theta \geqq 0$ and $H - \omega_1 \lambda_\theta \geqq 0$, then $\dot{p}(t_1) \leqq 0$

b) if $H \leqq 0$ and $H - \omega_2 \lambda_\theta \leqq 0$, then $\dot{p}(t_2) \geqq 0$

where $\omega_i = [\mu/r_i^3]^{1/2}$. As $p(t_1) = p(t_2) = 1$, it comes immediately that if $\dot{p}(t_1) > 0$, or $\dot{p}(t_2) < 0$, or both, $\max[p(t)] > 1$ and the trajectory can be declared nonoptimal without any further computation. Therefore, conditions a and b can be regarded as simplified necessary conditions for possible optimality.

In the general case, a numerical computation of $p(t)$ is necessary. Figure 6 shows typical primer magnitude histories corresponding to given area of the (τ, ϕ) plane. Figure 7 gives the complete domain of possible optimality for $\rho = 1.52$, as a result of a systematic computation. This domain cannot[13] include parts of the axes $\phi = \pm 2\pi$ and does not extend to infinity.

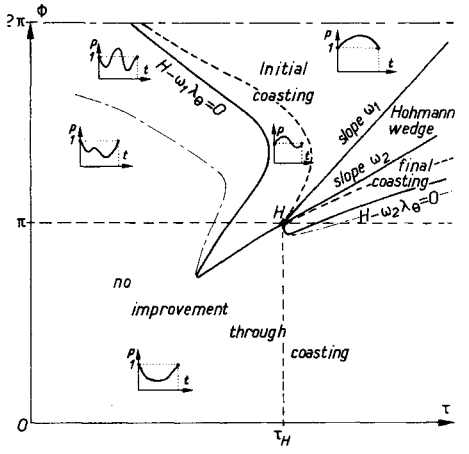

Fig. 6 Domains of improvement through terminal coasting.

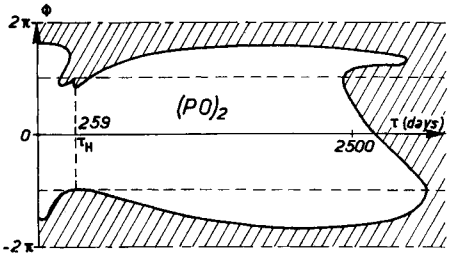

Fig. 7 Domain of possible optimality for two-impulse rendezvous.

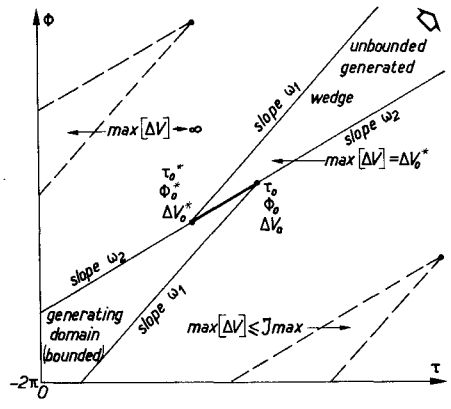

Fig. 8 Generating domain and generated wedge.

Terminal Coast and Two-Impulse Trajectories

If a coasting period is allowed on the initial or final orbit, candidate trajectories for a given set of data (τ_0, ϕ_0) are no longer unique. They belong to an infinite set of trajectories $(C)TC_0\,T(C)$, each corresponding to some $TC_0\,T$ trajectory. These $TC_0\,T$ trajectories fill a finite-surface domain, denoted "generating-domain" in Fig. 8 and to each generating trajectory corresponds some Δv. Within the generating domain, Δv's may or may not be upper bounded (they are if all τ's are >0) and may or may not take stationary values.

A variational approach to the choice of the least Δv generating trajectory was presented by Handelsman[8] so that candidate generating trajectories can be found at mutual intersection of loci $H-\omega_i\lambda_\theta=0$ or/and at the intersection of these loci with the boundaries of the generating domain. A maxima-minima approach would, in addition, check all the boundaries,[7] but, it will not be used here. Then, if no "variational candidate" is available, no coast is contemplated and the solution is the standard $TC_0\,T$ trajectory. Assuming, for τ_0 and ϕ_0, the proper generating trajectory found at $\tau_0{}^*$, $\phi_0{}^*$ (with a corresponding $\Delta v_0{}^*$), this selected trajectory belongs to the generating domains of all points (τ, ϕ) of an unbounded "generated wedge," as shown in Fig. 8, and $\Delta v_0{}^*$ is an upper bound for the characteristic velocity of $(C)TC_0\,T(C)$ trajectories in the wedge.

Let the domain where $(C)TC_0\,T(C)$ trajectories improve upon $TC_0\,T$ trajectories be referred to as "terminal coast domain." It is bounded by the loci $H-\omega_i\lambda_\theta=0$, as the presence of one of these in the generating domain has been declared necessary. In this domain, shown in Fig. 6, the function $\Delta v(\tau, \phi)$ is much affected. From what has been said concerning the generated wedge, equal $-\Delta v$ contours cannot close in on themselves, and actual contours are straight lines.[8] These remarks hold for any terminal coast domain disregarding the number of impulses of the generating trajectories. But the terminal coast domain should not be identified to $(PO)_{2+}$, for these can be $(C)TC_0\,T(C)$ trajectories improving upon $TC_0\,T$ but yet not as much as 3 or 4 impulse trajectories. Therefore, the possible optimality of $(C)TC_0\,T(C)$ trajectories has to be checked. To the $TC_0\,T$ part of such a trajectory corresponds a given primer vector $\Lambda(t)$; as seen above. A first necessary condition is therefore that $p(t)\leqq 1$, along this part, i.e., that $TC_0\,T\in(PO)_2$. The primer vector along the circular arc is defined by using two necessary conditions[6] so at the connecting impulse, $\Lambda^+=\Lambda^-$ and $\dot\Lambda^+=\dot\Lambda^-$. Here again, the only necessary condition which can be violated is that upon the primer magnitude along the coasting arc. As for the generating trajectory, it belongs to one of the loci $H-\omega_i\lambda_\theta=0$ which, for vacant terminals, partly belong to the border of $(PO)_2$, in the neighborhood of point H. Let points where these loci leave $(PO)_2$ be called "splitting points." Eligible generating must therefore belong to a curved segment going from H to one splitting point. Two straight lines issuing from these points are a first bound to the $(PO)_{2+}$ domain.

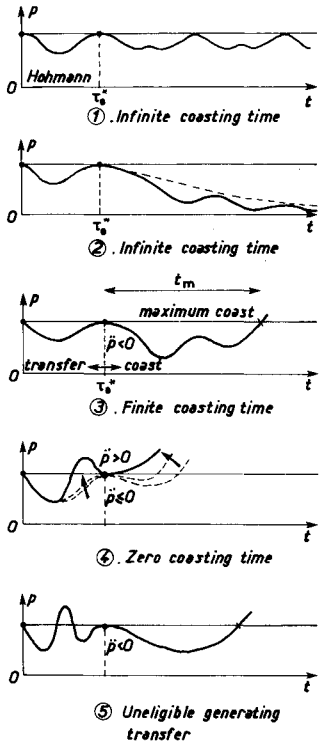

Fig. 9 Typical $p(t)$ histories for two-impulse $TC_0\,T$ trajectories.

Before $p(t)$ is computed on the circular arc, a first check can be made at the connecting impulse. Noting that [8,13]

$$H-\omega_i\lambda_\theta=0\Leftrightarrow\dot p(t_i)=0$$

the second derivative can be expressed as

$$\ddot p(t_i)=\Lambda^T(t_i)(\mathbf{G})\Lambda(t_i)+\dot\Lambda^T(t_i)\cdot\dot\Lambda(t_i)$$

if

$$\ddot p(t_i)>0,\quad p(t_i+|\varepsilon|)>1\quad\text{for}\quad 0<\varepsilon\ll 1.$$

and the circular arc is nonoptimal. The point where $\ddot p(t_i)=0$ on $H-\omega_i\lambda_\theta=0$, called here "extreme point," is another bound to eligible generating trajectories. But, as $\ddot p(t_i)>0\Rightarrow p(t_i-|\varepsilon|)>1.$, the extreme point is either identical to the splitting point or already outside $(PO)_2$. Therefore, it is not a constraining bound. It is yet a useful concept, as we shall see further. Assuming $\ddot p(t_i)\leqq 0$ there is necessarily a time ε during which all necessary conditions are met on the coasting arc, i.e. $p(t_i+\varepsilon)<1.$. In the general case, $p(t)\leqq 1.$ during a finite interval of time t_{mc} as illustrated in Fig. 9③. Boundary conditions at time t_i $[\Lambda(t_i)$ and $\dot\Lambda(t_i)]$ enable an easy computation of the maximum coasting time $t_{mc}=\omega_i{}^{-1}\phi_{mc}$, which in turn gives $\tau_{mc}=\tau_0{}^*+t_{mc}$, $\phi_{mc}=\phi_0{}^*+\phi_{mc}$. Any trajectory constructed with the generating trajectory $TC_0\,T(\tau_0{}^*, \phi_0{}^*)$ and a coasting arc larger than the defined maximum is nonoptimal and susceptible of improvement by use of an extra impulse. For a Hohmann-connected circular leg, t_{mc} can grow to infinity:[13] if $\rho<15.6$, $p(t)\leqq 1.$ for all t's with $p(t)=1$ when $t=2k\pi/\omega_i$ (Fig. 10 ①); if $\rho>15.6$, $p(t)>1$ when $t=k\pi/\omega_i$ and therefore $t_{mc}<\pi/\omega_i$. If the circular leg is connected to a near-Hohmann trajectory, set $\psi_i=\varepsilon\ll 1$ and

$$\Lambda(t_i)=(\varepsilon, 1-\varepsilon^2)$$

$$\dot\Lambda(t_i)=\chi_i(\varepsilon^2-1, \varepsilon)\quad\text{with}\quad\chi_i\gtrless 0$$

which can be expressed as

$$\chi_i=\chi_{iH}+k_1\varepsilon+0(\varepsilon^2),\qquad k_1\gtrless 0$$

and, for $\rho<15.6$, $p^2(2k\pi/\omega_i)=1-6\varepsilon(1+2r_i{}^3\chi_{iH})2k\pi+0(\varepsilon^2)$ with $k<0$ (>0) for an initial (final) coasting arc. As $\chi_{iH}>0$, $p^2(2k\pi/\omega_i)=1-6\alpha^2\varepsilon 2k\pi+0(\varepsilon^2)$ initial coast $\varepsilon=\psi_1<0$, $k<0$, final coast $\varepsilon=\psi_2>0$, $k>0$, therefore, $k\varepsilon>0$ and for $p^2(t)$ to be greater than one requires k of the order of ε^{-1}. When $\varepsilon\to 0$, $k\to\infty$ and $t_{mc}\to\infty$ (Fig. 9 ②).

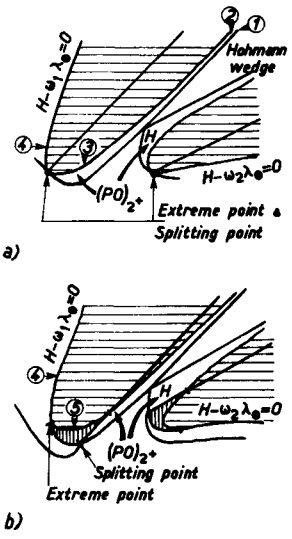

Fig. 10 Examples of domains of possible optimal coast (not to scale).

In all cases, t_{mc} takes its maximum value when the generating trajectory is in H and decreases to reach zero when the generating trajectory is at the extreme point. $(PO)_{2+}$ is thus bounded by 1) the loci $H-\omega_i\lambda_\theta=0$, 2) the Hohmann wedge (which can be cast apart), and 3) the computed limits (τ_{mc}, ϕ_{mc}). If the extreme point merges with the splitting point, as in Fig. 10a, these three boundaries define $(PO)_{2+}$. Should the two points be distinct, a fourth boundary would be found at the straight lines issuing from the splitting points, as shown in Fig. 10b. Numerical computations, for $\rho = 1.52$, could not separate the two points.

As a conclusion, if the total number of impulses is arbitrarily limited to two, terminal coasting enables substantial reductions of Δv over a large domain of the (τ, ϕ) space (Fig. 6). But as a solution to the general problem of n-impulse optimal rendezvous, $(C)TC_0\,T(C)$ trajectories are stationary in a strongly reduced domain $(PO)_{2+}$. It is divided in two distinct parts by the Hohmann wedge and goes to infinity for $\rho < 15.6$ (This result is similar to this of Prussing[10,11]) but for $\rho > 15.6$ both $(PO)_{2+}$ and the Hohmann wedge are bounded domains.

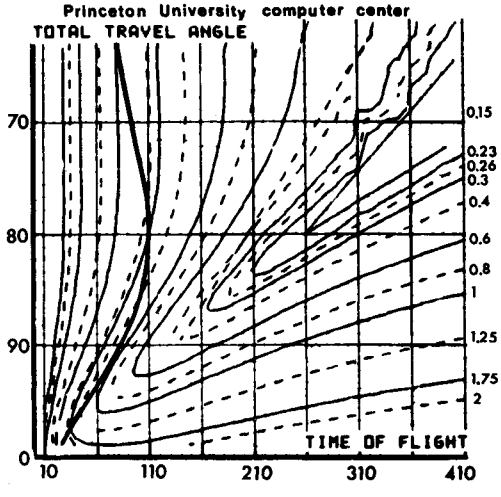

Fig. 11 Characteristic velocity for three-impulse trajectories (heavy line notes $E(\tau, \phi) = 0$).

Three-Impulse Trajectories

There is a three-dimensional infinity of three-impulse trajectories matching a set of data (τ, ϕ), among which there is no simple choice. In this three-dimensional space, there can be an indefinite number of maxima and minima for Δv. Position and timing of the middle impulse are arbitrary and make three independent variables which can be used to describe all possible solutions: for a given set of these variables, the problem is reduced to two Lambert's problems and the solution is unique. The question, then, is to find the minimum for Δv. Here again, there is no analytic solution available and numerical direct methods are necessary in order to solve this parametric optimization problem. Here a finite-difference second gradient method was used to determine $\Delta v(\tau, \phi)$ as shown in Fig. 11. Gradient methods require a starting trajectory. Wherever there exists a $TC_0\,T$ trajectory (i.e., when $|\Phi| \leqq 2\pi$), or a $(C)TC_0\,T(C)$ trajectory (i.e., when $-2\pi \leqq \phi \leqq \omega_1\tau + 2\pi$), which can be regarded as special cases of $TC_0\,TC_0\,T$ trajectories, they provide the required initial trajectory. Therefore, three-impulse solutions cannot but improve upon corresponding Δv's. (Note that it is not true in the Hohmann wedge where $CTC_0\,TC$ trajectories cannot be duplicated by some $TC_0\,TC_0\,T$ trajectory) and constant Δv contours for $TC_0\,TC_0\,T$ can therefore not be closed contours. In accordance with the theory, an improvement has been made upon the value of Δv everywhere outside of $(PO)_2$ and $(PO)_{2+}$. But, starting from the $TC_0\,T$ solution, the program has some difficulties in duplicating circular coasting arcs in $(PO)_{2+}$, near the Hohmann wedge. The obtained Δv is larger than what could be expected, and in general, there is nothing either to confirm or to disprove the uniqueness of the solution (for circular terminals). The radius at second impulse is shown in Fig. 12. To the left of the Hohmann wedge it is less than r_1, the theoretical value in the corresponding part of $(PO)_{2+}$. To the right of the wedge, it is larger than r_2.

Once the minimum $-\Delta v$ solution selected, the adjoint system is computed along both legs of the trajectory. For almost all computed primer magnitude histories, $\max[p(t)] > 1$. This, as well as jumps in the values of H and λ_θ computed separately on both legs, indicate the nonoptimality of the selected trajectories. However, if the arguments of the optimum Δv have not been found, the function itself is very close to its optimal value.[14] This shows the great sensitivity of the adjoint variables to nonoptimality. Recently, an analytical expression for the gradient in the parametric space has been presented,[9] using the primer vector analysis, and corresponding computational methods[14] are, by far, quicker and more efficient than standard direct methods.

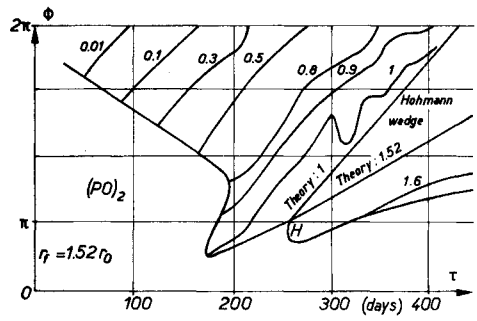

Fig. 12 Radius at middle-impulse of three-impulse $TC_0\,TC_0\,T$ trajectories.

Conclusion

A quantitative and qualitative description of the characteristic velocity corresponding to all two-impulse $TC_0\,T$ trajectories has been made. The domain of possible optimality for such trajectories has been computed which shows it is a closed domain. The effect of optional terminal coast is described and the domain in which they can be optimal is defined. It is a two-parts, narrow domain extending on both sides of the Hohmann wedge. As this wedge does, it goes to infinity (when $\rho < 15.6$) or not. Wherever the primer vector analysis gives two-impulse trajectories as nonoptimal, three-impulse trajectories have yielded some improvement upon Δv, and in that case only. However computations of $TC_0\,TC_0\,T$ trajectories have been neither accurate nor extensive

enough to enable the estimation of $(PO)_3$. This domain should not extend to infinity as four-impulse trajectories are necessary when $\phi > 4\pi$ and optimal when $\tau \to \infty$. A complete computation of $(PO)_3$ and $(PO)_4$ is called for to ascertain whether or not four impulses are sufficient in the nonlinear case.[15] Such are the questions left open about impulsive rendezvous, to say nothing of the uniqueness of the solutions found, which, in spite of the present results, can be questioned.[7]

References

[1] Lambert, J. H., *Insignores Orbitae Cometarum Proprietates*, Monograph, 1761, W. Engelmann, Leipzig, East Germany, 1902.

[2] Breakwell, J. V., Gillespie, R. W., and Ross, S., "Researches in Interplanetary Transfers," *ARS Journal*, Vol. 31, No. 2, Feb. 1961, pp. 201–208.

[3] Jordan, J. F., "The Applications of Lambert's Theorem to the Solution of Interplanetary Transfer Problems," TR 35.521, Feb. 1, 1964, Jet Propulsion Lab., Pasadena, Calif.

[4] Pines, S., "A Uniform Solution of Lambert's Problem," Internal Note 65 FM 166, Dec. 13, 1965, Manned Spacecraft Center, Houston, Texas.

[5] Battin, R. H., "A New Solution for Lambert's Problem," *Proceedings of the XIXth International Astronautical Congress*, Vol. 2, Pergamon, New York, 1970, pp. 131–150.

[6] Lawden, D. F., *Optimal Trajectories for Space Navigation*, Butterworths, London, 1963; also "Fundamentals of Space Navigation," *Journal of the British Interplanetary Society*, Vol. 13, No. 2, 1954, pp. 87–101.

[7] Peltier, J. P., "Étude numérique de l'optimalité des rendezvous bi-impulsionnels entre orbites planétaires (circulaires et coplanaires)," *La Recherche Aérospatiale*, No. 6, Nov.–Dec. 1970, pp. 291–300.

[8] Handelsman, M., "Some Necessary Conditions for Optimal Fixed-Time Powered Transfers with Multiple Coast and Thrust Between Circular Orbits," *Proceedings of the XVIIth I.A.F. Congress*, Madrid, Spain, Oct. 1966.

[9] Lion, P. M. and Handelsman, M., "The Primer Vector on Fixed Time Impulsive Trajectories," *AIAA Journal*, Vol. 6, No. 1, Jan. 1968, pp. 127–132.

[10] Prussing, J. E., "Optimal Four-Impulse Fixed-Time Rendezvous in the Vicinity of a Circular Orbit," *AIAA Journal*, Vol. 7, No. 5, May 1969, pp. 928–935.

[11] Prussing, J. E., "Optimal Two- and Three-Impulse Fixed-Time Rendezvous in the Vicinity of a Circular Orbit," *AIAA Journal*, Vol. 8, No. 7, July 1970, p. 1221.

[12] Marec, J. P., "Rendez-vous multi-impulsionnels, optimaux, de duré moyenne, entre orbites quasi-circulaires, proches, coplanaires," *Proceedings of the XIXth International Astronautical Congress*, Vol. 2, Pergamon Press, New York, 1970, pp. 173–200.

[13] Peltier, J. P., "Investigation about some Impulsive Trajectories for Optimal Rendezvous," AMS Rept. 916c, July 1970, Aerospace Systems Lab., Princeton Univ., Princeton, N.J.

[14] Minkoff, M. and Lion, P. M., "Optimal Multi-Impulse Rendezvous Between Trajectories," *Proceedings of the XIXth International Astronautical Federation Congress*, New York, Oct. 1968.

[15] Edelbaum, T. N., "How many Impulses?," *Astronautics and Aeronautics*, Vol. 5, No. 11, 1967, pp. 64–69.

APRIL 1972 AIAA JOURNAL VOL. 10, NO. 4

Orbital Eccentricity and Angular Momentum Management Scheme Stability

RONALD A. MAYO*
The Bendix Corporation, Navigation and Control Division, Denver, Colo.

The class of angular momentum management schemes considered in this paper consists of a large attitude maneuver followed by a sequence of trim maneuvers. The characteristic equation is derived for general momentum sampling, switching logic, and system gains. The satellite orbital parameters are assumed arbitrary and in the neighborhood of the reference orbit. For a specific sampling scheme, the sampled momentum by the *n*th orbit is shown to converge to the sum of the classical Neumann series on momentum space augmented by the initial CMG cluster momentum. For small eccentricity, a linear (first order in eccentricity) management scheme stability analysis is presented. These studies are combined in a derivation of the range of eccentricity for which the continuous time CMG momentum remains bounded within the saturation limit of the momentum exchange device for arbitrary angular position of perigee. The results are extended to allow variation in the mean orbital radius.

Nomenclature

$K(a, \varepsilon, \theta_p)$	= linear operator on momentum space
$g(a, \varepsilon, \theta_p)$	= disturbance momentum accumulation per orbit after first orbit; sampling scheme (2)
$\tilde{g}(a, \varepsilon, \theta_p)$	= disturbance momentum accumulation for first orbit only; sampling scheme (2)
$(a, \varepsilon, \theta_p)$	= true orbital parameters
A, B, C	= control functions (switching logic and system gains) dependent on θ
θ	= angular position of vehicle in orbital plane with respect to $\hat{X}_R$
g_0	= acceleration of gravity at R_0
R_0	= mean radius of Earth
r	= distance from Earth's center to center of mass of vehicle
$\hat{r}$	= unit vector directed from center of Earth to center of mass of vehicle
I	= inertia tensor of vehicle
$M_\theta, M_\varepsilon, M_0$ M_t, M_{cf}	= linear operators on momentum space
M_{jk}	= linear operator having representation with respect to $\hat{X}_v, \hat{Y}_v, \hat{Z}_v$ axes consisting of all zeros except (j, k) element which equals one
$\Phi(\theta)$	= transition matrix on momentum space
$F^*(z), C^*(z)$	= 3×3 transition matrices in z-transform domain
$Q(a, \varepsilon, \theta_p)$	= $\int M_\theta(dt/d\theta)d\theta$ linear operator on momentum space; $\int$ denotes integration on desaturation period $[(2n + 1)\pi, 2(n + 1\pi)$; $Q(a, \varepsilon, \theta_p)$ is independent of n
$\tilde{\pi}$	= uncontrollable vector torque (independent of control functions) during desaturation period
$M_\theta H_0(2n\pi)$	= controllable vector torque (dependent on control functions) during desaturation period
$H_e(\theta)$	= error momentum; sum of disturbance momentum plus controllable vector momentum
$\oint$	= integration over complete orbit
$\hat{X}_R, \hat{Y}_R, \hat{Z}_R$	= ATM reference system (Fig. 1 and Fig. 2)
$\hat{X}_b, \hat{Y}_b, \hat{Z}_b$	= principal axes of satellite inertia tensor
$\hat{X}_v, \hat{Y}_v, \hat{Z}_v$	= vehicle axes; the principal axes are coincident with the vehicle axes only during experimental hold mode
$\|\cdot\|$	= the Euclidean norm on momentum space

Received July 6, 1971; revision received November 22, 1971.
Index categories: Manned Space Station Systems; Spacecraft Mission Studies and Economics; Spacecraft Attitude Dynamics and Control.

* Project Engineer, Guidance and Control Systems.